



Spatio-temporal trend of crop phenology, SPEI, and their interactions over different agro-ecological regions of India

Mamta Kumari¹ · Abhishek Chakraborty¹ · Vishnubhotla Chakravarathi² · Parth Sarathi Roy³

Received: 7 March 2023 / Accepted: 3 July 2023 / Published online: 11 July 2023
© The Author(s), under exclusive licence to Springer-Verlag GmbH Austria, part of Springer Nature 2023

Abstract

The study focuses on analyzing the impact of dryness/wetness, derived from Standardized Precipitation Evapotranspiration Index (SPEI), on vegetation phenology in different agro-ecological zones (AERs) of India during 2001–2018. Long-term CRU TS3 SPEI datasets at a 3-month time scale were used to characterize the drought events, while Normalized Difference Vegetation Index (NDVI) data from MODIS at a 250 m scale was used to extract crop phenology metrics. The results revealed that the dryness was prevalent in the hot sub-humid regions since the new millennium. Non-parametric trend analysis showed that northeast India experienced the highest increase in drought events over the past 38 years. In terms of phenology metrics, approximately 59, 23, and 61% of agricultural areas displayed an increasing trend of the start of season (SoS), seasonal NDVI amplitude (NDVI_{max}), and length of season (LoS). However, 21% of agricultural area showed a decreasing trend in SoS, 5.17% in NDVI_{max}, and 28% in LoS. The impact of climate extremes varied across different AERs, that too in dry and wet years. During drought years, most AERs exhibited a delayed SoS, reduced NDVI_{max}, and decreased LoS. The sensitivity of LoS to dryness is higher in semi-arid and sub-humid regions compared to arid and humid regions. Under the projected increase in extreme events, understanding resilient crop growth in response to dryness/wetness is crucial for adaptation and mitigation strategies. The findings of this study help in identifying areas that are particularly vulnerable to drought events and can contribute in informed decision-making.

1 Introduction

A significant increase in global mean air temperature has recently been reported by the Intergovernmental Panel on Climate Change (IPCC) sixth assessment report (IPCC 2021), leading to intensified extreme rainfall and drought events in south Asia. Chakraborty et al. (2017) have reported a significant warming trend and an increase in the extreme hot events over India. These changes have diverse impacts on society and ecosystems, varying across different regions based on their vulnerabilities (Parsons et al. 2019).

Amid the different types of droughts, agricultural drought is one of the complex hazards where soil moisture is limited to support crop growth (Dalezios et al. 2014; Wilhite and Buchanan-Smith 2005). The agricultural drought has pronounced effect on rainfed regions, which is prevalent in India occupying nearly two-thirds of agricultural land (Rao et al. 2015; Sathyan et al. 2018). Agricultural productivity in these areas is heavily influenced by climatic factors, viz., rainfall and evapotranspiration (Mall et al. 2006). Previous studies have primarily focused on the effect of temperature or rainfall on crop growth, rather than the impact of drought on crops (Hatfield and Prueger 2015). Drought indices, such as Standardized Precipitation Index (SPI), Palmer Drought Severity Index (PDSI), and Standardized Precipitation Evapotranspiration Index (SPEI), are valuable indicators for analyzing and interpreting drought severity (McKee et al. 1993; Palmer 1965; Vicente-serrano et al. 2010). However, these indices have certain limitations. For example, PDSI requires comprehensive water balance components, making it data-intensive and restricted in use (Zhai et al. 2010; Li et al. 2015). SPI, based on long-term rainfall data, can lack consistency, especially in arid regions with

✉ Abhishek Chakraborty
jeet.abhishek@gmail.com

¹ Agriculture Sciences and Applications Group, Remote Sensing Applications Area, National Remote Sensing Centre, Balanagar, Hyderabad, Telangana 500037, India

² Centre for Earth, Ocean and Atmospheric Sciences, University of Hyderabad, Gachibowli, Hyderabad, Telangana 500032, India

³ Sustainable Landscapes and Restoration, World Resources Institute India, New Delhi 110016, India

high evaporation demands (Pramudya and Onishi 2018; Mishra and Singh 2011). In contrast, SPEI overcomes these limitations by incorporating rainfall and evapotranspiration data, making it useful indicator for monitoring wet and dry events (Tirivarombo et al. 2018; Chen and Sun 2017). SPEI is sensitive to changes in climatic demand of evaporation (Beguería et al. 2014) and can act as a proxy for soil moisture (Ahmad et al. 2018; Das et al. 2021).

Recent studies revealed that the croplands are the major contributor to greening in India, while forests have a minor contribution (Parida et al. 2020; Chen et al. 2019). While previous studies have examined vegetation dynamics in India, they focus on forests at the national and regional levels (Ranjan and Gorai 2022; Jeganathan et al. 2010; Kumar et al. 2022; Chakraborty et al. 2018a), neglecting explicit analysis of croplands. Crop phenology, which expresses the seasonal events of plant processes, is a crucial indicator of crop growth pattern changes in response to climate change. Understanding crop phenology is crucial as changes in crop phenology can impact carbon accumulation, crop yield, crop duration and distribution of diseases, and other environmental and social aspects (Richardson et al. 2009). Remote sensing provides a synoptic overview of crop-growing regions, enabling regular monitoring of crop growth, health, and productivity. Remote sensing cannot directly identify a particular crop growth stage or phenological events due to coarse spatial resolution of satellite data, resulting into mixed spectra, particularly from heterogeneous grid. Therefore, a more generalized phenology, i.e., “land surface phenology” metrics (pheno-metrics), is computed (de Beurs and Henebry 2005) which indicates the seasonality change in spectral observation and depicted as SoS, LoS, and NDVI at peak stage, etc. Previous research have examined the influence of climate change on crop growth and crop yield in India, demonstrating the varying relationship between crop growth patterns and drought (Malhi et al. 2021; Arora 2019; Kumar and Gautam 2014; Guntukula 2020; Rai and Apoorva 2020). Several studies are carried out to explore the temporal pattern of phenology metrics using satellite data derived Normalized Difference Vegetation Index (NDVI) time series in wetlands (Shen et al. 2023), forests (Friedl et al. 2014; Liu et al. 2020; Wang et al. 2020), croplands (Anwar et al. 2015; Ishtiaq et al. 2022; Ge et al. 2021; Javed et al. 2021; Yang et al. 2021), and grasslands (Shen et al. 2022) in different parts of the world. However, sparse studies are available analyzing the impact of dry/wet events on crop phenology, especially in a country like India. Limited researches (Chakraborty et al. 2014; Chakraborty et al. 2018b; Das et al. 2020) utilized 8-km GIMMS NDVI3g data to analyze the trend in phenology and its association with rainfall. These studies have exploited meteorological unit-level boundary or state-administrative boundary to represent the findings that do not capture the variability in agricultural

area and patterns within an India’s heterogeneous landscape characterized by small land holdings.

While a few studies have addressed the cropland phenology using high-resolution MODIS or Landsat, they have been limited to specific areas; and focused on production or vegetation condition anomaly (Kumar et al. 2022; Bhavani et al. 2017, Singh and Sanatan 2021). Notably, there is lack of studies that address impact of dryness/wetness on crop phenology at the agro-ecological region (AER) level for the entire country. AER represents homogenous land unit in terms of climatic, soil, and physiography which accounts the heterogeneity in agriculture. This study aims to fill this gap by comprehensive and fine scale evaluation of the impact of dry/wet events on crop phenology at AER level.

In a nutshell, the study involves analysis of the impact of climate warming-induced drought on vegetation phenology in various agro-ecological regions of India from 2001 to 2018. This analysis was performed using SPEI with a 3-month time scale (SPEI-03) along with phenological metrics. The objectives of this study are to (1) analyze the spatio-temporal pattern of SPEI-03 and phenological metrics across India, (2) quantify the impacts of dry and wet events on crop phenology in the study area, and (3) explore the relationship between SPEI-03 and phenology metrics during the study period in the Indian region. By examining these objectives, the study aims to provide valuable insights into the effects of climate change-induced drought on vegetation and agricultural systems in India.

2 Study area

The study was carried out over 20 AERs of India (Fig. 1). The AERs have continuously large agricultural land areas and each AER is extracted out of a climatic zone, correlated with landforms, climate, and the length of growing period (Subramaniam 1983). The crop phenology in each AER could easily be identified using time series satellite data. Here, the length of growing period represents the number of days when moisture is available for crop growth. Each AER is homogenous in terms of physiography, type of climate, length of growing period, and soil types for macro-level agricultural land-use planning. Table 1 summarizes the characteristics of different AERs in India.

3 Data used and methodology

The schematic diagram of the methodology followed in the present study is shown in Fig. 2.

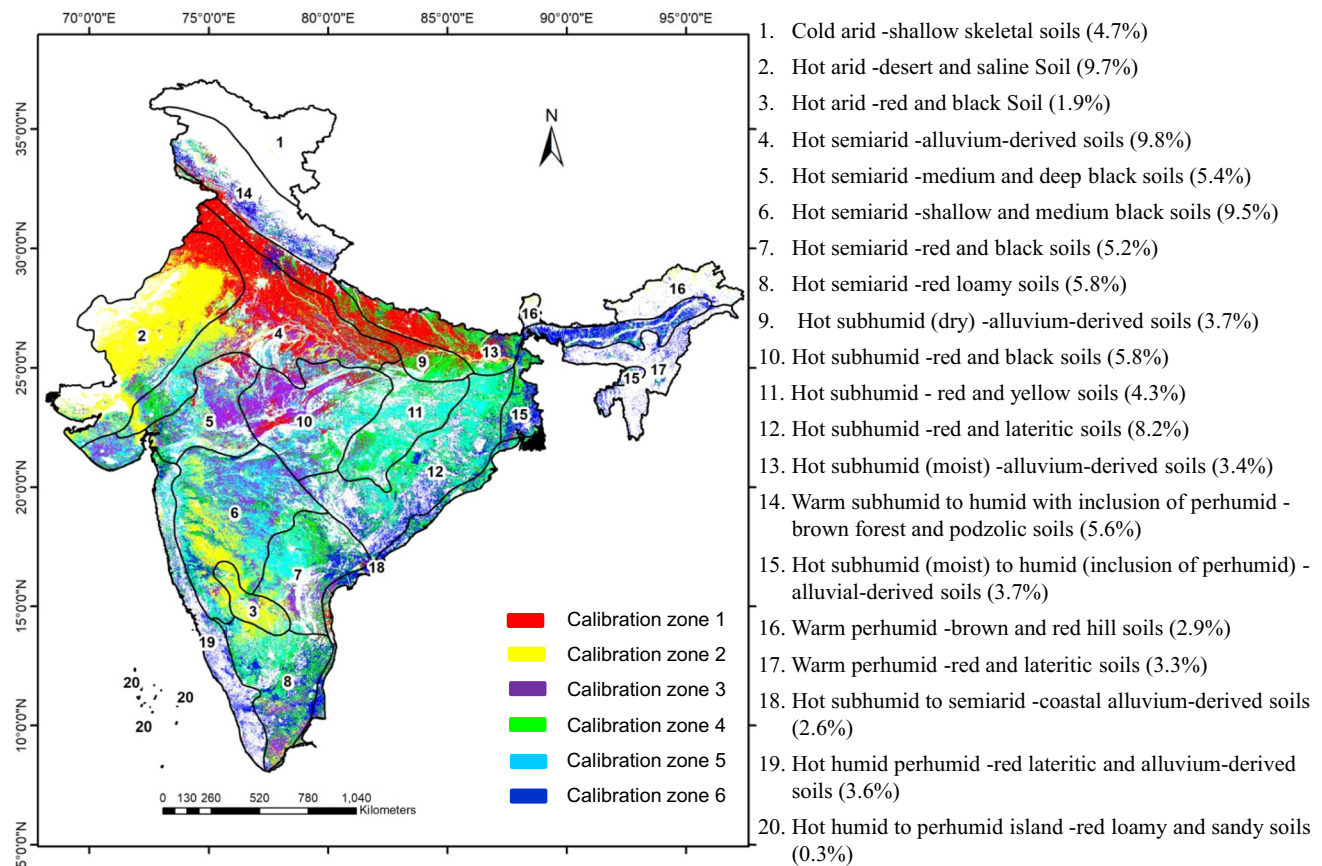


Fig. 1 Study area encompassing agro-ecological regions (AERs) of India representing dominant climate and soil types along with 06 calibration zones (values inside brackets depict percentage of geographical area falling in each AER)

3.1 Meteorological data

The long-term SPEI data were obtained from the Global SPEI database. The database, available at http://spei.csic.es/spei_database, provides SPEI data at a spatial resolution of $0.5^\circ \times 0.5^\circ$ on monthly basis for an extended period of time. For this particular study, SPEI data at a 3-month time scale (SPEI-03) of version 3.2 Climatic Research Unit (CRU) dataset were used for southwest monsoon season months (June, July, August, and September) spanning from 1981 to 2018. The SPEI can be classified into different wet/dry conditions, as shown in Table 2 (Nam et al. 2015).

3.2 Processing of MODIS NDVI time series

This study analyzed 250 m spatial resolution Moderate Resolution Imaging Spectroradiometer (MODIS) NDVI product (MOD13Q1 v006) from 2001 to 2018. The 16-day maximum value composite approach reduced cloud cover, allowing for capturing local crop phenology variations.

The study utilized TIMESAT software to extract crop phenology metrics (pheno-metrics) from the NDVI time

series (Jonsson and Eklundh 2004; Eklundh and Jönsson 2017). Due to significant variability in agricultural practices across the Indian subcontinent, a data-driven approach is adopted by dividing India into different calibration zones. To determine the appropriate smoothing techniques and associated zone-specific parameter settings in TIMESAT, principal component analysis (PCA) was employed on the time series NDVI data (Heumann et al. 2007). PCA is a statistical technique used to reduce the dimensionality of data. Multiple-year land use land cover maps (NRSC 2014) were used to extract potential agricultural areas in India.

To implement PCA, NDVI images for the first fortnight (i.e., first 15 days) of each month in 2006, 2013, and 2017 were selected. These years were considered as “normal” years and were representative of typical crop growth periods. The first four principal components were used to extract six calibration zones (Fig. 1) using ISODATA clustering technique. The fact that these four PCs explain over 95% of the variance in the data indicates that they capture a significant portion of the important information in the NDVI images. The Savitsky–Golay filter (Chen et al. 2004) and double logistic function (Tan et al. 2010) were applied with

Table 1 Characteristics of various agro-ecological regions of India

AER	Geographical area (gross cropped area) (million ha)	Physiography	Precipitation (PET) (mm)	Length of growing period (days)	Major crops growing in AER
AER-01	15.2 (0.07)	Western Himalayas	< 150 (<800)	< 90	Vegetables, millets, wheat, fodder, pulses
AER-02	31.9 (20.85)	Western Plain and part of Kachchh Peninsula	< 300 (1500–2000)	< 90	Millets, fodder, pulses
AER-03	4.9 (4.18)	Deccan Plateau	400–500 (1800–1900)	< 90	Sorghum, cotton, oilseeds, sugarcane
AER-04	32.2 (30.05)	Northern Plain and Central Highlands including parts of Gujarat Plains	500–800 (1400–1900)	90–150	Millets, wheat, pulses, maize, cotton, and sugarcane
AER-05	17.6 (11.04)	Central (Malwa) Highlands, Gujarat Plains, and Kathiawar Peninsula	500–1000 (1600–2000)	90–150	Millets, wheat, pulses
AER-06	31.0 (25.02)	Deccan Plateau	600–1000 (1600–1800)	90–150	Millets, cotton, pulses, sugarcane
AER-07	16.5 (6.19)	Deccan Plateau (Telangana) and Eastern Ghats	600–1000 (1600–1700)	90–150	Millets, oilseeds, rice, cotton, & sugarcane
AER-08	19.1 (6.96)	Eastern Ghats (Tamil Nadu uplands) and Deccan Plateau (Karnataka)	600–1000 (1300–1600)	90–150	Millets, pulses, oilseeds, sugarcane, and rice
AER-09	12.1 (11.62)	Northern Plain	1000–1200 (1400–1800)	150–180	Rice, wheat, pigeon pea, sugarcane, mustard, maize
AER-10	22.3 (14.55)	Central Highlands (Malwa and Bundelkhand)	1000–1500 (1300–1500)	150–180	Rice, wheat, sorghum, soybean, pulses
AER-11	11.1 (6.47)	Eastern Plateau (Chhattisgarh Region)	1200–1600 (1400–1500)	150–180	Rice, millets, wheat, pulses
AER-12	26.8 (12.09)	Eastern Plateau (Chhotanagpur) and Eastern Ghats	1000–1600 (1400–1700)	150–180	Rice, pulses, millets
AER-13	11.1 (10.95)	Eastern Plains	1400–1600 (1300–1500)	180–210	Rice, wheat, sugarcane
AER-14	18.2 (3.20)	Western Himalayas	1600–2000 (800–1300)	180–210	Wheat, millets, maize, rice
AER-15	12.1 (8.99)	Bengal and Assam Plain	1400–2000 (1000–1400)	> 210	Rice, jute, plantation crops
AER-16	9.6 (1.37)	Eastern Himalayas	2000–4000 (<1000)	> 210	Rice, millets, potato, maize, oilseeds
AER-17	10.6 (1.56)	North-eastern Hills	1600–2600 (1000–1100)	> 210	Rice, millets, potato, plantation crops
AER-18	8.5 (6.12)	Eastern Coastal Plains	900–1600 (1200–1900)	90–210	Rice, coconut, pulses, oilseeds
AER-19	11.1 (5.70)	Western Ghats and Coastal Plains	2000–3200 (1400–1600)	> 210	Rice, tapioca, coconut, spices
AER-20	0.8 (0.05)	Islands of Andaman-Nicobar and Lakshadweep	1600–3000 (1400–1600)	> 210	Rice, coconut, areca nut, oil palm

various parameter settings (seasonality, envelope adaptation strengths, and window sizes) to denoise the NDVI profiles within each calibration zones. Please be informed that the calibration zone was delineated to capture areas with similar pattern of temporal NDVI profiles for implementing zone-specific setting of the fitted equation.

3.3 Extraction of crop phenology metrics

The method described by Jönsson and Eklundh (2004) is used to extract phenology metrics in this study. Specifically,

TIMESAT software is employed to fit a curve to the NDVI time series and extract the following pheno-metrics: (a) start of season (SoS): The time point when the NDVI value of the fitted curve first exceeds the 0.2 times value of distance between the minimum and maximum NDVI values on the rising side. It signifies the onset of crop growth during the monsoon season; (b) season maximum NDVI amplitude ($NDVI_{max}$): The difference between the maximum NDVI and the base NDVI values. $NDVI_{max}$ represents the magnitude of the NDVI increase during the growing season; (c) length of growing season (LoS): The duration between the SoS

Fig. 2 Schematic diagram of the methodology followed in the present study

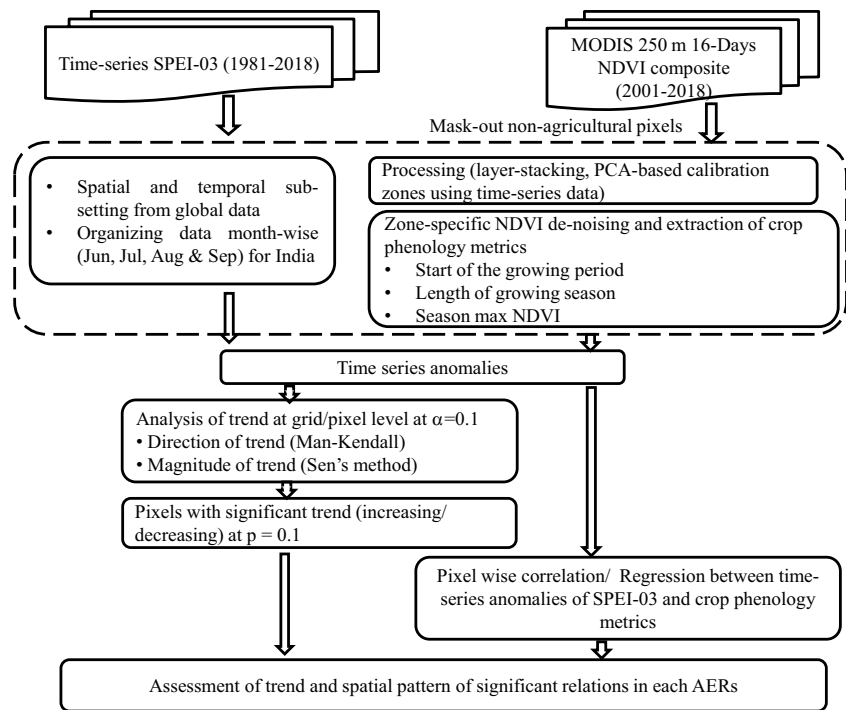


Table 2 Classification of dryness/wetness condition based on SPEI (Nam et al. 2015)

Condition	SPEI class	Condition	SPEI class
Extreme drought	$SPEI \leq -2$	Mild wet	$0.5 < SPEI \leq 1$
Severe drought	$-2 < SPEI \leq -1.5$	Moderate wet	$1 < SPEI \leq 1.5$
Moderate drought	$-1.5 < SPEI \leq -1$	Severe wet	$1.5 < SPEI \leq 2$
Mild drought	$-1 < SPEI \leq -0.5$	Extreme wet	$SPEI \geq 2$
No drought	$-0.5 < SPEI \leq 0.5$		

and the end of the season, which is the point in time when the NDVI value falls below the 0.2 times value of distance between the minimum and maximum NDVI values on the falling side of curve. LoS indicates the length of time the crop experience active growth.

3.4 Calculation of temporal trends of SPEI-03 and crop phenology metrics

In this study, anomalies of the crop phenology metrics (SoS, LoS, and $NDVI_{max}$) are computed by subtracting the long-term mean from each year’s value at both the pixel and AER level. The anomalies show the deviation of pheno-metrics from their typical values over time. Mann–Kendall test (Mann 1945; Kendall 1976), a widely used non-parametric statistical test for trend detection in environmental time

series data, was used for trend analysis. The Mann–Kendall test compares the ranks of each observation with those of all other observations to assess whether there is a significant increasing or decreasing trend over time. In addition to detecting significant trends, Sen’s method (Sen 1968) was used to estimate the magnitude of the trend. Sen’s method is a non-parametric technique that calculates the median slope between all pairs of observations, providing a robust estimate of the trend magnitude. Pixel-wise Mann–Kendall test ($p = 0.1$) for the time series anomalies of SoS, LoS, and $NDVI_{max}$ was performed for the null hypothesis of no trend against the alternative hypothesis of decreasing/increasing trend. On a similar line, trend analysis was carried out for time series SPEI-03 data for June, July, August, and September.

3.5 Relating SPEI-03 and crop phenology metrics

Pearson’s correlation analysis was used to investigate the temporal relationships with monthly SPEI-03 of four monsoon months and phenological metrics. Generally, crop phenological events in an area are primarily determined by the climatic conditions preceding the events (Shen et al. 2014; Güsewell et al. 2017). The anomalies of time series SPEI-03 and crop phenology metrics were brought to 50 km spatial resolution for 2001–2018.

This study analyzed the spatial patterns of significant correlations ($p = 0.1$) to gain the insight into how changes in rainfall affect crop phenology (SoS, LoS, and $NDVI_{max}$). Sensitivity analysis was performed between the phenology

metrics and SPEI-03 of individual months in the monsoon season. The sensitivity analysis was performed across the twenty different AERs of India. The sensitivity of each AER was defined as the change in phenology metrics per unit change in SPEI-03, i.e., slope of the regression model between phenology metrics and SPEI-03 over 2001–2018.

4 Results and discussion

4.1 Zone-wise temporal characteristics of SPEI-03

The average SPEI-03 for the entire country of India during the period 1981–2018 is presented in Fig. 3. Wet events ($SPEI \geq 0.5$) and dry events ($SPEI \leq -0.5$) were calculated for each monsoon months (June to September) during the same period for each AER and are summarized in Table 3. Additionally, the entire time series (1981–2018) was divided into four decades to compute the percentages of occurrence

of dry, wet, and normal ($0.5 > SPEI > -0.5$) events for each specific month, as shown in Fig. 4.

Figure 3 clearly shows that wet and dry events based on SPEI-03 are well distributed across the time series (1981–2018). Notably, the severity of the dry events are found to be more pronounced in the later part of the time series, particularly during the initial part of the twenty-first century. Conversely, the frequency and intensity of wet events were observed to be higher towards the end of the time series (2006–2018).

Based on the monthly frequency of occurrence of wet ($SPEI > 0.5$) and dry ($SPEI < 0.5$) events, the AERs were classified into three categories: wetting, drying, and mixed. AERs 2, 3, 4, and 14 exhibited a higher occurrence of wet events compared to dry events during the period 1981–2018 and are classified as “Wetting” regions. These AERs predominantly cover the hot/warm, arid regions of India. Conversely, AERs 10, 11, 13, 15, and 17 displayed a “Drying” pattern with more dry events than wet events. These AERs

Fig. 3 Temporal variation of SPEI-03 (year 1981–2018) of India

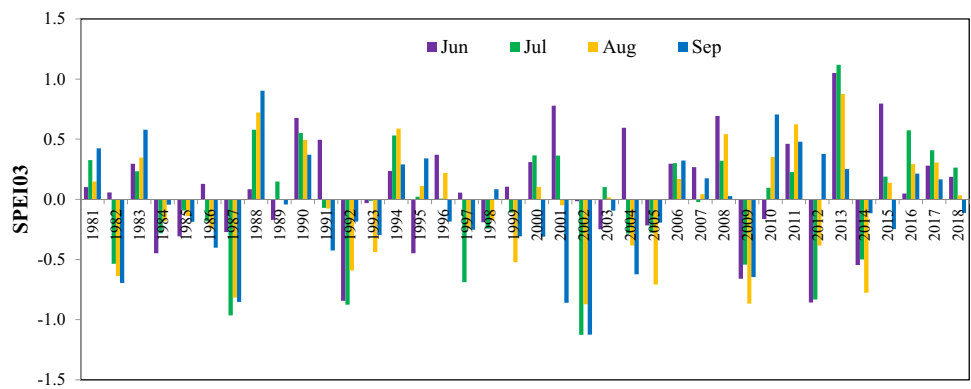
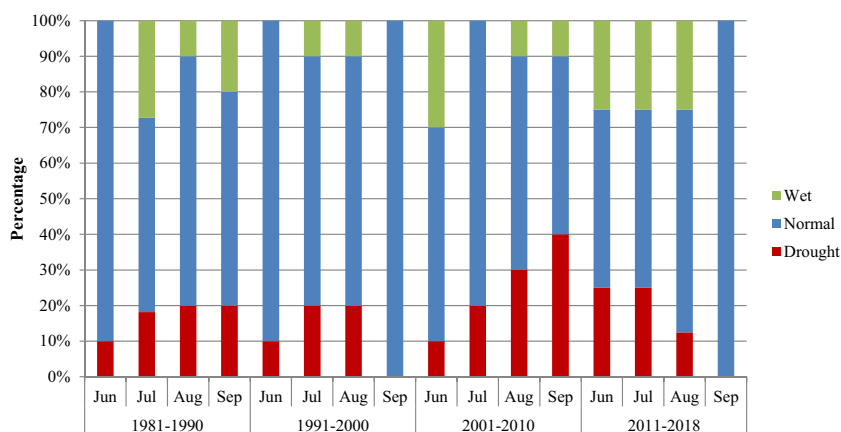


Table 3 Distribution of dry ($SPEI-03 \leq 0.5$) and wet ($SPEI-03 \geq 0.5$) month counts in each AER over the monsoon months (June–September) during 1981–2018

	AER	June		July		August		September	
		Wet	Dry	Wet	Dry	Wet	Dry	Wet	Dry
Wetting	2	13	10	9	8	11	7	9	8
	3	17	10	13	11	13	11	12	15
	7	12	12	12	9	11	7	13	10
	14	20	2	21	7	17	11	9	9
Mixed	4	15	6	12	11	8	10	7	12
	5	9	9	9	11	13	9	13	11
	6	8	8	8	12	11	11	12	14
	9	15	7	11	12	6	15	5	17
Drying	8	7	13	11	9	11	11	12	10
	19	9	11	9	8	10	11	12	9
	10	10	13	10	16	5	15	7	16
	11	9	12	9	16	5	17	4	21
	13	8	10	8	14	4	20	7	16
	15	10	15	5	11	8	18	10	13
	17	11	17	7	13	6	17	9	15

Fig. 4 Frequency (%) of occurrence of wet, normal, and drought events during different decades from 1981 to 2018 based on SPEI-03



are primarily located in hot sub-humid regions of India. The remaining AERs showed mixed results.

The decade-wise analysis of monthly occurrence of wet, dry, and normal events, as depicted in Fig. 4, reveals that drought events (dry) were evenly distributed in the first decade (1981–1990). However, there was a shift in the distribution of dry events in the subsequent decades. Notably, the frequency of late-season drought was high during 2001–2010, whereas early-season drought was more prevalent in the last decade (2011–2018).

In general, the majority of the extreme drought events occurred between 2001 and 2010, consisting 10%, 20%, 30%, and 40% for the months of June, July, August, and September, respectively. No drought was observed during September of 1991–2000 and 2011–2018, while the other months experienced dry spell in all decades. In the decade of 2001–2010, almost all the months of SW monsoon exhibited drought incidences (early, mid, and late seasons). However, the frequency of dry spells mostly coincided with the reproductive/maturity growth stage of crops due to the onset of late-season drought. Early-season drought was found to be more prevalent in the decade 2011–2018.

4.2 Spatial variations of temporal trends of SPEI-03

The spatial distribution of the temporal trends of SPEI-03 during SW monsoon months is illustrated in Fig. 5. Pixel-wise trend was estimated using Mann–Kendall statistics. Further, Sen’s method was used to estimate the magnitude of the trend (positive/negative) at pixel level. Pixels having statistically significant trend at $p = 0.1$ were marked as “*” as shown in Fig. 5. Positive trends indicate an increase in wet events, while negative trends indicate an increase in drought events.

In June, a significant positive trend in SPEI-03 (at $p = 0.01$) was observed in parts of northern India, the eastern coastal parts of central and southern India, and isolated patches in the north-eastern part of India (AER 03, AER

07, AER 14, and AER 18). On the contrary, a significant negative trend was observed in the lower parts of the north-eastern India (AER 15) during June. In July, a significant positive trend in SPEI-03 was observed in the central and southern parts of India (AER 03, AER 05, AER 10, AER 12, and AER 18), while a significant decreasing trend was found in the north-eastern part (AER 15 and AER 17). The trend analysis of August month revealed scattered patches of increasing trends in AER 05, AER 06, AER 08, and AER 11, and decreasing trends in AER 15 and AER 17 across India. In September, the entire north-eastern part of India exhibited a negative trend in SPEI-03 indicating an increase in drought events in this region (AER 15, AER 17), despite being a high rainfall zone. Some areas of central and peninsular India showed an increasing trend in September SPEI-03 (AER 03, AER 05, AER 06, AER 08, and AER 11). Overall, the trend analysis results indicated that northeast India (a high rainfall zone) experienced the greatest increase in drought events over the past 38 years, whereas central India had the lowest increase (Fig. 5). In general, wet events have significantly increased across India. This information is valuable for understanding the impact of changing rainfall and temperature patterns on different areas and can be utilized to develop strategies for mitigating climate-related impacts on agriculture in these regions.

Table 4 presents the AER-wise percentage of grids exhibiting positive/negative trends in SPEI-03 during 1981–2018, along with the mean magnitude of these trends during the monsoon months. AERs with a significantly high trend ($> 0.5 \text{ years}^{-1}$) over more than 50% of the grid are marked in bold italics. It is evident from Table 3 that AERs 3, 7, 14, and 18 displayed a positive trend over a large area with a magnitude of $0.5\text{--}1.14 \text{ year}^{-1}$ during the month of June. Similarly, during July, a positive trend of $0.56\text{--}0.73 \text{ year}^{-1}$ was observed over a significantly large area in AERs 3, 5, 10, 12, and 18. AER 8 showed a high positive trend ($0.52\text{--}0.57 \text{ year}^{-1}$) over the majority of the grid in August. In September, AERs 3, 5, and 8 also exhibited a high

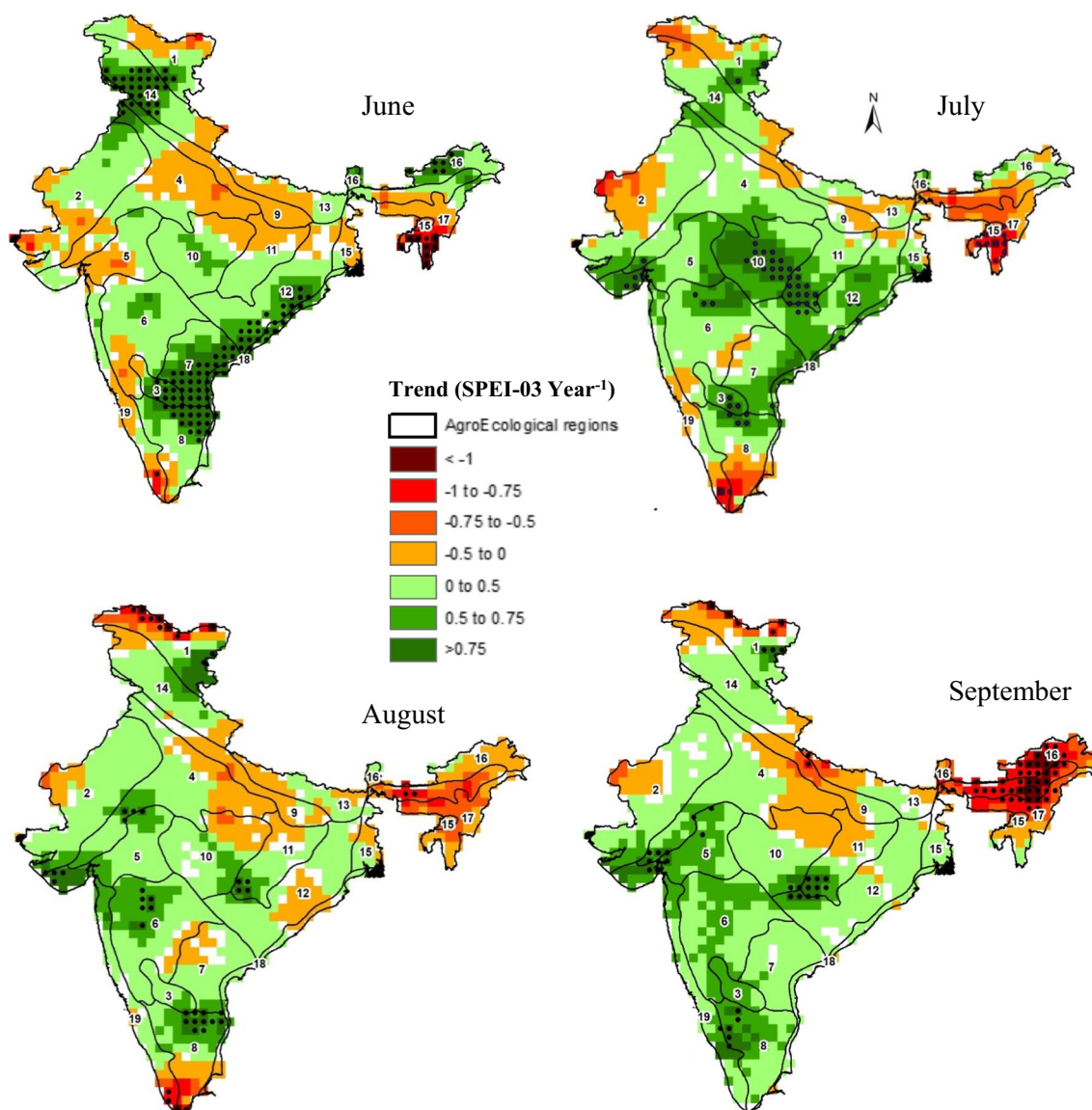


Fig. 5 Spatial patterns of temporal trends of SPEI-03 across the monsoon months (June, July, August, and September) during 1981–2018. Grids with significant trend (positive/negative) at $p = 0.1$ are represented with black dots

positive trend in the lion's share of the grid. A significantly high negative trend ($0.5\text{--}0.8\text{ year}^{-1}$) is observed over large contiguous areas of AERs 15 and 17 during July–September. The present findings are in agreement with the findings of Das et al. (2014) and Das et al. (2020).

In summary, the Indian peninsula, specifically the eastern coastal region and the upper western coastal region, exhibited a significant trend of increasing wetness. Conversely, the north-eastern region, known for its high rainfall levels and biodiversity hotspots, demonstrated a significant drying trend. It is noteworthy that a substantial portion of the upper-central part of India, the Indo-Gangetic plain, often referred to as the country's food basket, displayed a drying trend, although it did not reach statistical significance at the $p = 0.1$ level.

4.3 Spatial patterns of temporal trend of crop phenology metrics over India

The spatial distribution of the temporal trends in crop phenology metrics (SoS, NDVI_{\max} , LoS) during the southwest monsoon season was analyzed at 250-m spatial resolution using time series NDVI data from 2001 to 2018, employing the Mann–Kendall method. The analysis excluded AERs 01, 16, and 20 due to negligible agricultural activity. The resulting spatial patterns of temporal trends of the phenology metrics are presented in Fig. 6.

An increasing trend ($>1\text{ day/year}$) in SoS, indicating a delay in sowing activities during the monsoon season, was observed across large parts of the country, including

Table 4 AER-wise percentage of grid under positive/negative trend of SPEI-03 during 1981–2018 along with its mean magnitude over the monsoon months.

AERs	Jun			Jul			Aug			Sep						
	Positive		Negative	Positive		Negative	Positive		Negative	Positive		Negative				
	Grid (%)	Mean trend	Grid (%)	(-) trend	Grid (%)	Mean trend	Grid (%)	Mean trend	Grid (%)	Mean trend	Grid (%)	Mean trend				
2	44.1	0.27	23.5	-0.05	52.9	0.26	39.2	-0.29	55.9	0.31	14.7	0.02	38.2	0.30	16.7	-0.13
3	56.3	1.14	37.5	-0.31	82.1	0.62	0.0	0.00	93.8	0.47	0.0	0.00	91.0	0.57	0.0	0.00
4	36.7	0.18	42.9	-0.26	88.8	0.36	3.1	-0.19	75.5	0.27	13.3	-0.26	72.4	0.24	15.3	-0.33
5	28.3	0.28	47.2	-0.12	90.2	0.56	0.0	0.00	88.7	0.46	0.0	0.00	88.7	0.56	0.0	0.00
6	68.8	0.29	12.9	-0.04	82.8	0.41	10.8	-0.13	83.9	0.39	0.0	0.00	93.5	0.49	0.0	0.00
7	56.5	0.76	0.0	0.00	89.1	0.49	5.5	-0.15	49.1	0.33	18.2	-0.02	92.7	0.25	0.0	0.00
8	57.9	0.63	26.3	-0.18	56.1	0.47	38.6	-0.49	63.2	0.56	29.8	-0.36	98.2	0.52	0.0	0.00
9	15.8	0.37	71.1	-0.24	44.7	0.24	36.8	-0.14	2.6	0.08	60.5	-0.21	15.8	0.18	65.8	-0.25
10	80.3	0.35	9.9	-0.15	89.3	0.73	0.0	0.00	66.2	0.30	15.5	-0.19	70.4	0.33	19.7	-0.21
11	53.3	0.25	33.3	-0.18	91.1	0.46	2.2	-0.04	55.6	0.37	20.0	0.01	46.7	0.48	40.0	-0.05
12	80.7	0.48	3.6	-0.02	91.6	0.57	4.8	-0.07	63.9	0.21	13.3	-0.14	77.1	0.32	2.4	0.15
13	15.6	0.21	68.8	-0.02	40.6	0.16	40.6	-0.08	25.0	0.08	59.4	-0.08	28.1	0.07	46.9	-0.32
14	68.4	0.50	7.0	-0.27	64.9	0.40	28.1	-0.22	52.6	0.33	14.0	-0.13	54.4	0.24	8.8	-0.15
15	45.9	0.17	24.3	-0.21	32.4	0.26	56.8	-0.52	24.3	0.05	56.8	-0.54	24.3	0.29	56.8	-0.86
17	11.4	0.45	54.3	-0.41	5.7	0.20	80.0	-0.63	0.0	0.00	68.6	-0.48	0.0	0.00	68.6	-0.63
18	64.7	0.76	0.0	0.00	64.7	0.64	11.8	-0.31	35.3	0.20	29.4	-0.24	52.9	0.24	0.0	0.00
19	0.0	0.00	7.3	0.05	48.8	0.33	39.0	-0.50	4.9	0.39	7.3	-0.14	14.6	0.59	0.0	0.00

AERs with significant trend (positive/negative) in > 50% of grids are shown as bold italic

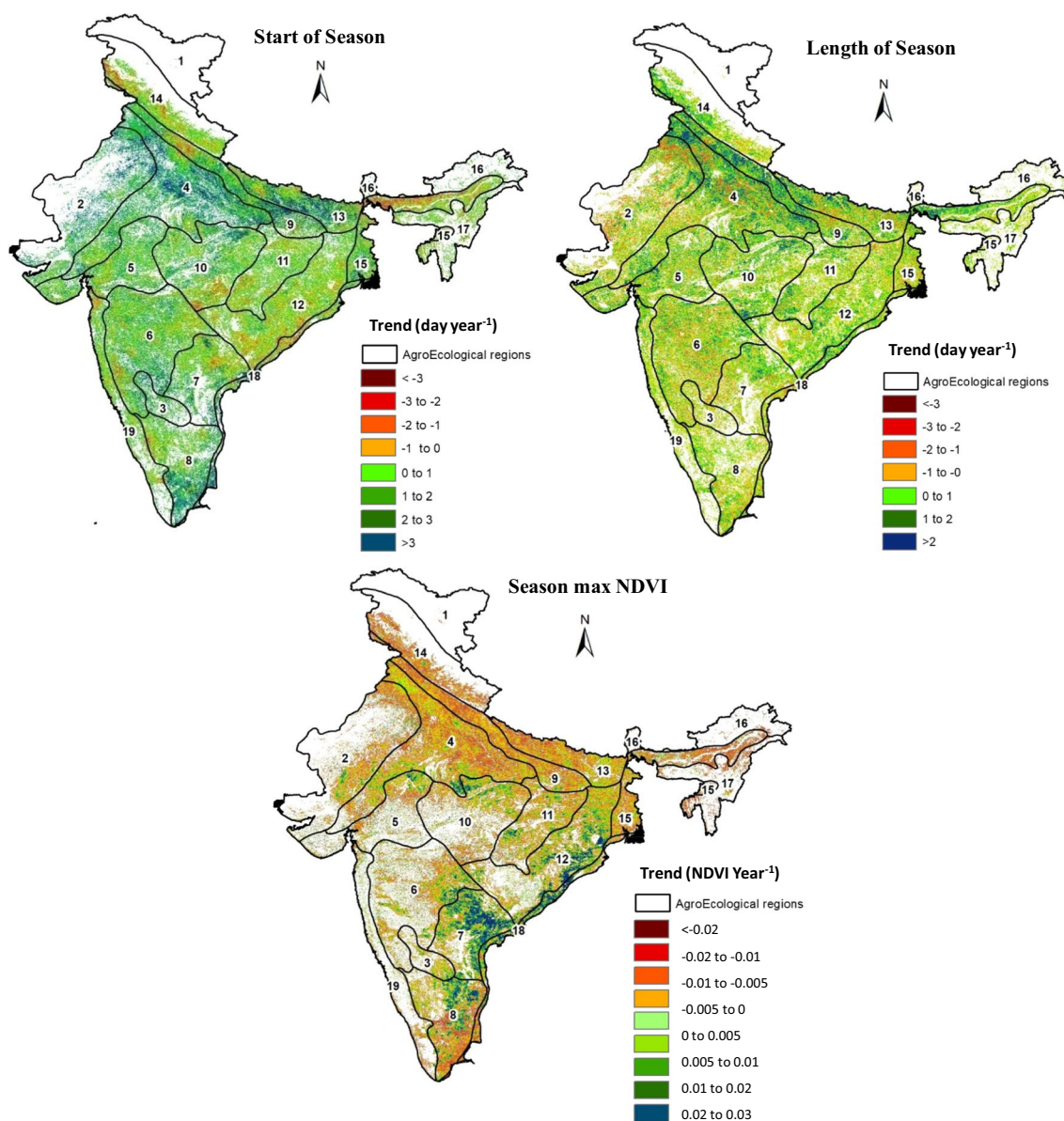


Fig. 6 Spatial patterns of temporal trends of crop phenology metrics (SoS, LoS, $NDVI_{max}$) in different AERs during 2001–2018

north, northwest, and Deccan plateau regions (AER 04, AER 02, AER 08, AER 09, and AER 13). Conversely, a pre-occurrence of sowing activities or a decreasing trend (<-1 day/year) in SoS was found in certain parts of the northern, central, and eastern India (AER 14, AER 12, and AER 10). Previous research studies examining spatio-temporal trends in phenology across India (Chakraborty et al. 2014; Das et al. 2020) or specific regions like the Indo-Gangetic plain (Sehgal et al. 2011; Chakraborty et al. 2018b) have reported divergent findings. These discrepancies arise from variations in the time period considered, spatial resolution of the data, choice of fitting function and pheno-metrics retrieval algorithms, and the aggregation of

the results based on administrative or climatic boundaries. However, majority of these studies have reached a consensus that SoS trend is increasing significantly in many parts of India. In the present study, it was found that approximately 59% of agricultural areas exhibited an increasing trend in SoS while 21% showed a decreasing trend. It is apt to mention here that the highest proportion of AER 04 (64%) experienced a delay in the SoS, whereas a pre-occurrence of SoS was noted in nearly 31.7% of the area in AER 09.

The spatial patterns of temporal trends of $NDVI_{max}$ (crop vigor) during the monsoon season (as shown in Fig. 6) revealed a decreasing trend over large contiguous areas in

the north, east, central, west, and south of India (AER 14, AER 04, AER 09, AER 13, AER 15, AER 08, and AER 02). Conversely, an increasing trend of $NDVI_{max}$ was observed in the central and southern regions of India (AER 07, AER 12, AER 18, AER 08, and AER 10). The central part of India, characterized by vertisols or black soil with high water holding capacity, might be experiencing changes in $NDVI_{max}$ trend due to improved crop management practices (irrigation, fertilization, plant protection, etc.) or the introduction of new crops in the region. Approximately 23.3% of the agricultural area exhibited a positive trend in $NDVI_{max}$, while only 5.17% displayed a decreasing trend. The region with the highest percentage of area experiencing increasing trends in $NDVI_{max}$ was AER 07 (33.1%), while AER 09 had the highest percentage of area with decreasing trends (24.25%). The spatial analysis of temporal trends in LoS (shown in Fig. 6) revealed increasing trends (>1 day/year) in a significant portion of the northern, eastern, and some parts of central regions of India. In contrast, decreasing trends (<-1 day/year) were observed in certain areas of the western, central, and southern parts. Approximately 61% of the agricultural area exhibited an increasing trend in LoS, while 28% displayed a decreasing trend. The regions with the highest percentage of area under increasing and decreasing trend in LoS were AER 09 (73.1%) and AER 02 (38.12%), respectively.

In a study conducted by Das et al. (2020), utilizing 8-km GIMMS NDVI data, it was concluded that a significant portion of India experienced a decreasing trend in LoS. However, Chakraborty et al. (2018b), using 4-km STAR-global vegetation health products-NDVI, found an increasing trend in LoS. In the current study, the analysis of 250-m MODIS data also revealed an increasing trend of LoS across a major part of India. It is important to note that these studies differed not only in spatial resolution of satellite data but also

in the time series considered. Despite some scattered discrepancies, the findings of the current study align with other reported studies conducted in various regions of India.

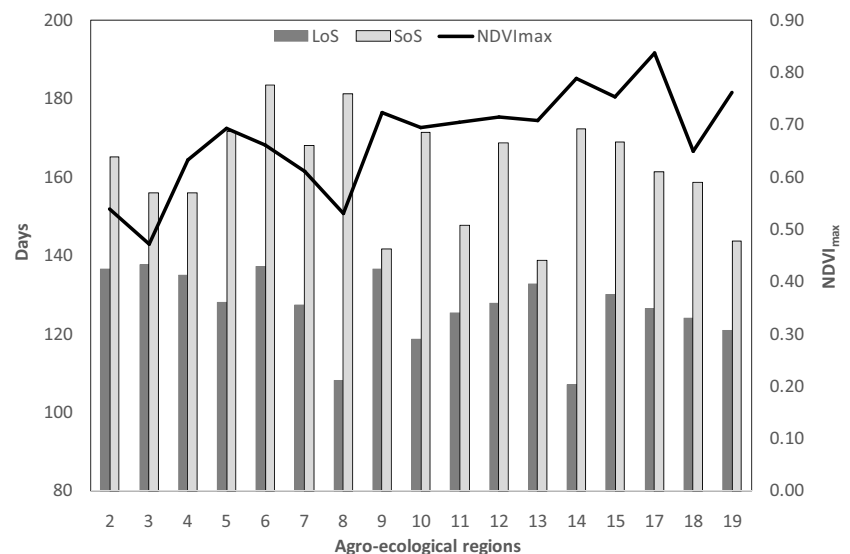
4.4 Influence of drought and wet years on crop phenology metrics

AER-wise mean phenology metrics (i.e., SoS, LoS, and $NDVI_{max}$) based on 250-m MODIS NDVI data of 2011–2018 are given in Fig. 7. Results revealed substantial variation in phenology metrics among the different AERs. There was no consistent relationship found between AER-wise mean pheno-metrics. For instance, early SoS coincided with long-duration LoS in AER 09, whereas short-duration LoS was associated with late SoS in AER 08. The mean $NDVI_{max}$ also exhibited extensive divergence among different AERs, with higher values observed in AERs 10–17 and lower values in AERs 2, 8, 9, and 19.

To assess the sensitivity of the pheno-metrics to SPEI-03, two contrasting years, namely 2012 and 2013, were selected based on overall dryness/wetness conditions. The year 2012 was characterized by dry conditions, while 2013 experienced wet conditions according to India Meteorological Department (IMD) and National Agricultural Drought Assessment and Monitoring System (<https://www.ncfc.gov.in/nadams>). Spatial maps of monthly SPEI-03 during 2012 and 2013 in Fig. 8 clearly illustrate the contrasting wetness conditions with moderate to severe drought prevailing in most areas of India during June to August 2012 and moderate to severe wetness dominating during the monsoon months of 2013.

These dry and wet conditions during the monsoon months may have influenced crop phenology by altering the crop-growing environment. AER-wise mean crop phenology

Fig. 7 AER-wise mean SoS (Julian day), LoS (number of days), and $NDVI_{max}$ over 2001–2018



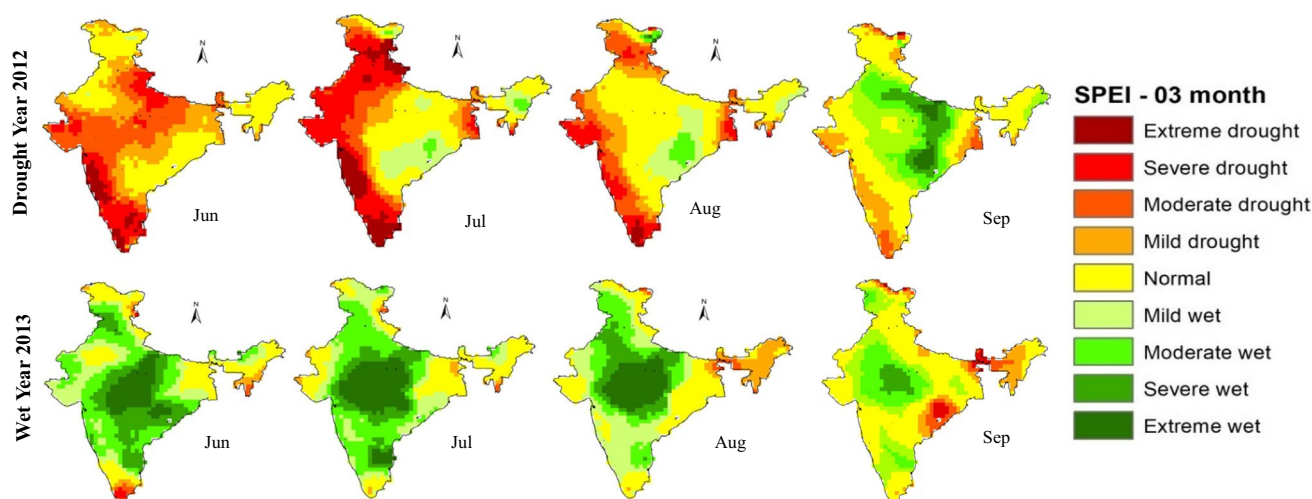


Fig. 8 Spatial pattern of SPEI-03 of monsoon months during drought (2012) and wet (2013) years

metrics (SoS, LoS, and $NDVI_{max}$) during drought and wet years demonstrated the impact of climatic extremes on crop phenology across different AERs. In dry conditions, SoS exhibited delays in sowing activities and emergence, LoS showed a decrease in the length of the crop-growing period, and $NDVI_{max}$ displayed reduced seasonal amplitude. These effects may be attributed to the selection of short-duration crops or failed sowing due to inadequate soil moisture availability. The temporal pattern of AER-wise phenology metrics is graphically represented in Fig. 9, and the spatio-temporal pattern is depicted in Fig. 10. These comparisons revealed that climatic variations significantly affect crop phenology. In 2013, there was generally an advancement of SoS ($\Delta SoS = -25 \pm 28$ days), while a slight delay of SoS was observed during 2012 ($\Delta SoS = 44 \pm 23$ days). $NDVI_{max}$ also exhibited reduced amplitude during drought year compared to wet year. The AERs, which showed minimum changes in phenometrics between 2012 and 2013, are climatic resilient. This may be due to high irrigation potential, water holding capacity of the soil, or prevailing cropping pattern.

4.5 Relationship between SPEI-03 and crop phenology metrics

4.5.1 Correlations between SPEI-03 and agricultural activities

The Pearson correlation coefficient (at $p = 0.1$) was calculated to assess the influence of wet and dry conditions on crop phenology metrics by analyzing the relationship between SPEI-03 and crop phenometrics. Figure 11 presents pixel-wise correlation between monthly SPEI-03 and the phenometrics. Several factors, such as the introduction of new crop type or crop variety, irrigation, and crop

management practices, may contribute to changes in crop phenology metrics, in addition to climate variations across different AERs. Around two-thirds of the country's agricultural land in India is under rainfed, making southwest monsoon rainfall crucial factor in agricultural productivity. The spatio-temporal distribution of rainfall and the climatic water demand govern crop growth and development, making SPEI-03 a potentially attributing factor to crop phenology during the monsoon season.

The start of the crop-growing season is determined by crop sowing activities, which is influenced by soil moisture availability during the early part of the season, mainly determined by the onset of rainfall. In India, the southwest monsoon typically begins in June, and the timely onset of monsoon significantly impacts crop sowing operation, especially under rainfed conditions. Delayed onset or insufficient rainfall during the early monsoon season leads to delay in crop sowing operations. Consequently, negative SPEI-03 during the early monsoon season results in positive anomalies in the start of season, indicating a delay in SoS, and vice-versa. A significant negative correlation between SoS and June rainfall was observed in large areas of India, highlighting the critical role of June rainfall in the timely onset of the crop season (Fig. 11). However, this relationship diminishes as the monsoon progresses into July and August. The LoS is also dependent on the timely start of the crop season. Therefore, June month's SPEI-03 also positively correlates with LoS over large areas of India. Correlation analysis between the SPEI-03 and SoS revealed a significant negative correlation in June and July, primarily concentrated in the central and northern parts of India (AER 10, AER 11, and AER 14).

The $NDVI_{max}$, which represents crop vigor, may be subject to change due to variations in crop type/varieties

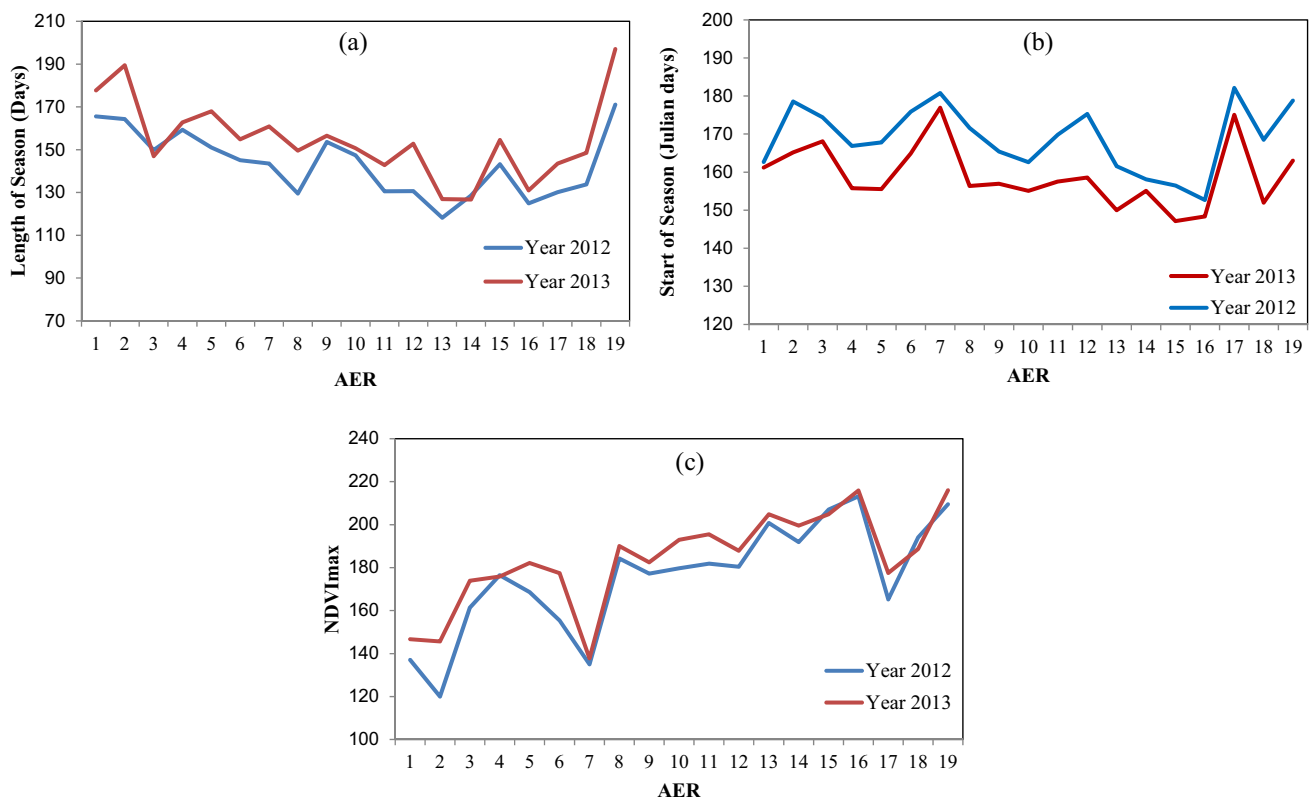


Fig. 9 Temporal pattern of pheno-metrics in wet and dry years for each AER: **a** LoS, **b** SoS, and **c** NDVI_{max}

within the study area. An increase in SPEI-03 (indicating wetter conditions) was found to correlate positively with NDVI_{max}, with a correlation coefficient greater than 0.5. Monsoon crops generally reach their peak vegetation phase in August–September. Timely sowing followed by well-distributed rainfall becomes critical for achieving high crop vigor (NDVI_{max}). Accordingly, June month’s SPEI-03, which is crucial for SoS, showed a positive correlation with NDVI_{max} over large areas of India. Similarly, August month’s SPEI-03 demonstrated a strong correlation with NDVI_{max} across India. The analysis revealed that the majority of AERs exhibited the maximum NDVI values in August–September, with the largest area (23%) showing a significant positive correlation with August month’s SPEI-03 (Fig. 11). For the relationship between SPEI-03 and pheno-metrics, we combined statistically significant pixels ($p = 0.1$) in June, July, and August across the study area (Fig. 12). The results indicate a uniform spread of significant correlation (positive/negative) between SPEI-03 and SoS/LoS throughout India. However, areas exhibiting a significant correlation between SPEI-03 and NDVI_{max} are predominantly concentrated in AER 2 and AER 5, highlighting the crucial impact of wetness/dryness on the agriculture in these regions of India. Previous studies have primarily focused on analyzing the spatio-temporal variation of either rainfall or

temperature on vegetation phenology (Fu et al. 2018; Kang et al. 2018; Chakraborty et al. 2014). Furthermore, the findings from other studies have demonstrated that croplands are particularly sensitive to climatic variability (Javed et al. 2021; Felton et al. 2019). Consequently, the current study investigated the impact of dry and wet climatic variability on crop phenology. The significant aspect of this study lies in exploring the effects of drought and wetness specifically during the months of the crop-growing season. In contrast to most previous studies (Potopová et al. 2015; Liu et al. 2018), this study focuses on examining the relationship between drought and pheno-metrics during the actual cropping season, rather than considering the entire annual calendar.

4.5.2 Sensitivity of pheno-metrics with SPEI-03

Table 5 provides the sensitivity of the phenology metrics to monthly SPEI-03 across different AERs. The slope in the table represents the change in the magnitude of pheno-metrics (expressed in “days” for SoS and LoS) per unit change in SPEI-03. Our observations indicate that a one-unit increase in SPEI-03, i.e., indicating greater wetness, leads to an early SoS of 01 to 18 days depending on the AERs. Almost all the AERs exhibit a pre-occurrence of SoS with increasing wetness (Table 5). The pre-occurrences of SoS was particularly

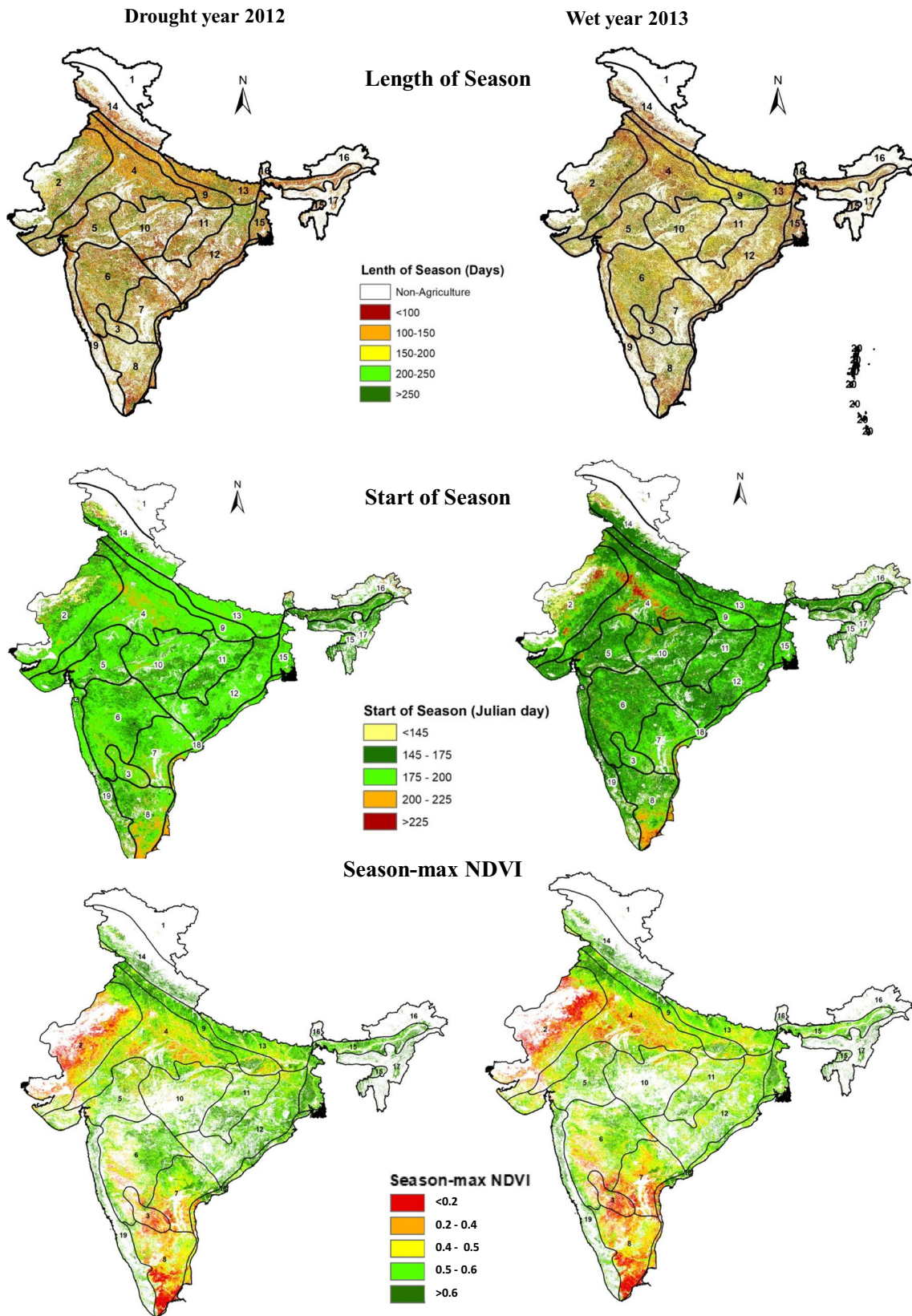


Fig. 10 Spatial pattern of pheno-metrics (LoS, SoS, and NDVI_{max}) in dry (2012) and wet (2013) years in each AER

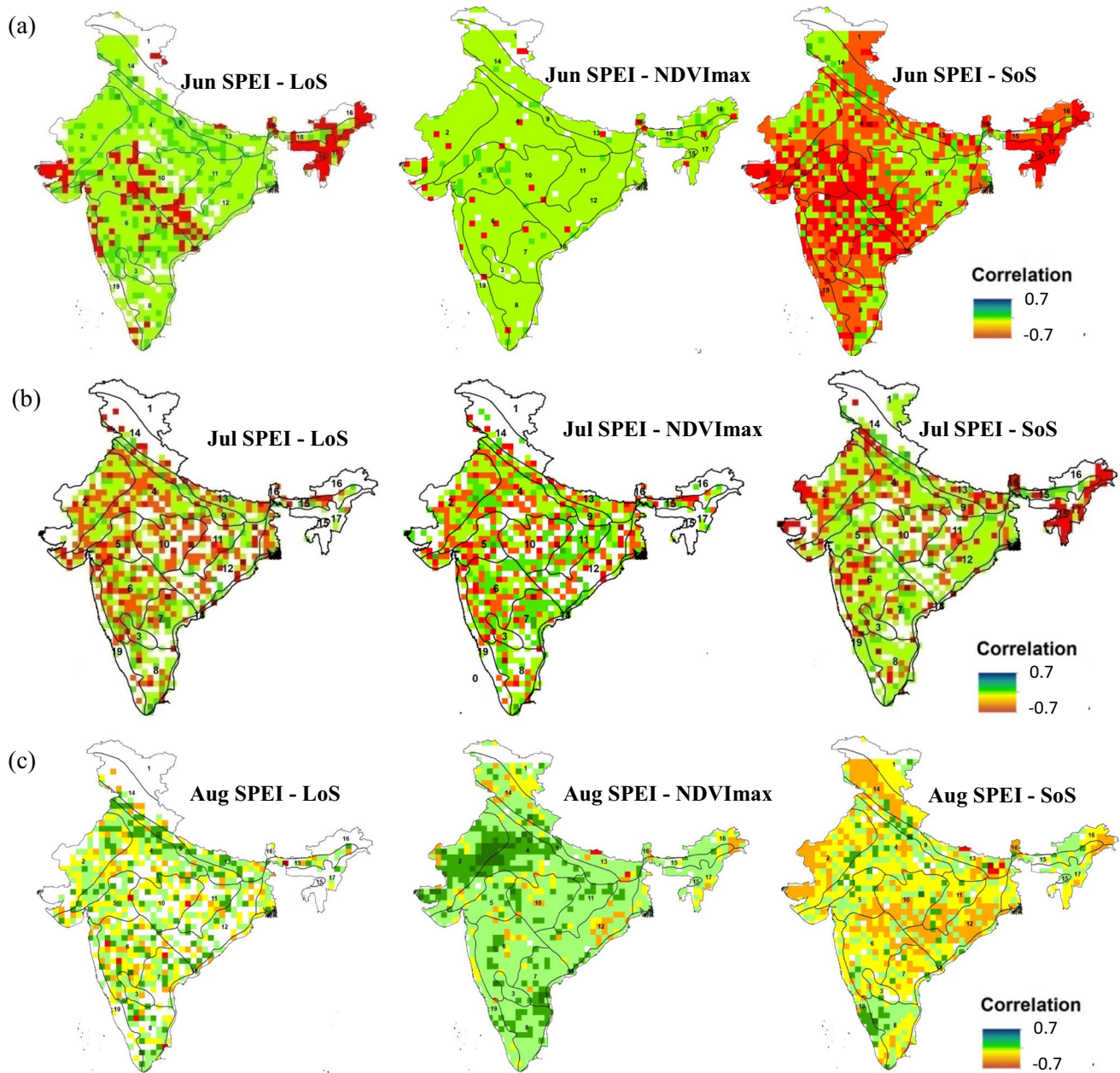


Fig. 11 Correlation between SPEI-03 vs phenology metrics (LoS, $NDVI_{max}$, and SoS): **a** June, **b** July, and **c** August months

noticeable in semi-arid regions with black soils (AERs 03, 04, 05, 06, 07) due to their high moisture holding capacity, as well as in humid/sub-humid AERs such as 13, 14, 15, and 17. Conversely, semi-arid climates with red lateritic soils (AERs 08, 09, 11, 12), characterized by poor water holding capacity, showed little or no change in SoS.

Similarly, increased moisture availability resulted in an extended length of the crop-growing period. Abundant soil moisture availability may trigger the farmers to select water-demanding crops with longer duration. The sensitivity of LoS to wetness varied across different climatic regions.

Humid/sub-humid climates showed negative or no sensitivity of LoS to increase in wetness, while semi-arid AERs exhibited an increase in LoS with greater SPEI-03. LoS sensitivity increased from arid to semi-arid regions (AER 02 to AER 08) and decreased from semi-humid to humid regions (AER 10 to AER 19). In July and August, $NDVI_{max}$ also displayed positive sensitivity to increase wetness, indicating high crop vigor in response to greater soil moisture availability across most of the AERs. We noted that the effect of dryness/wetness on SoS is more pronounced than LoS, consistent with the findings of Ge et al. (2021).

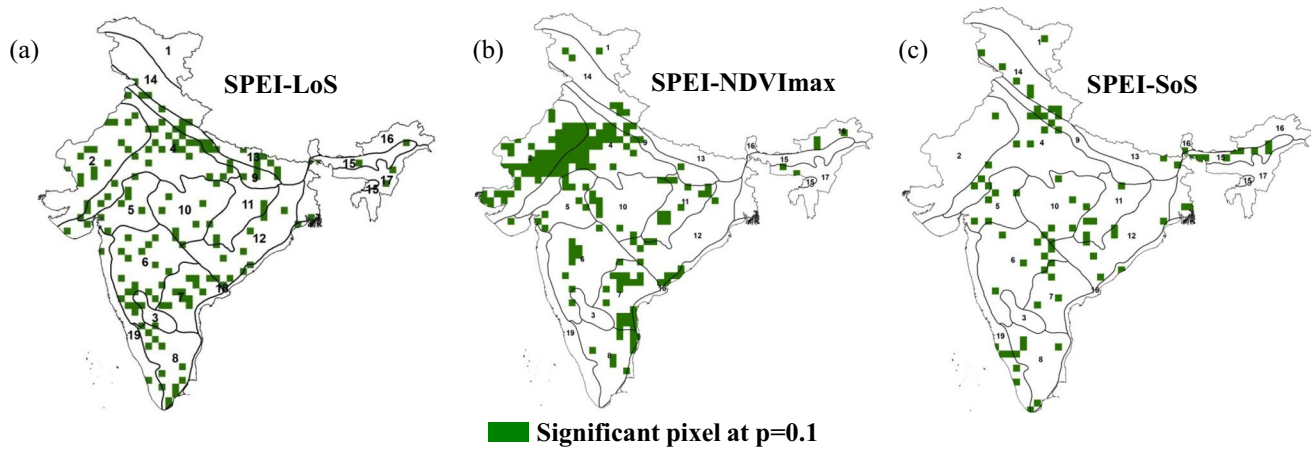


Fig. 12 Combined statistically significant pixels ($p = 0.1$) in June, July, and August months over study area for SPEI-03 and phenological metrics relation: **a** SPEI-03 and LoS, **b** SPEI-03 and $NDVI_{max}$, and **c** SPEI-03 and SoS

Table 5 Sensitivity of SoS, LoS, and $NDVI_{max}$ with SPEI-03 over different AERs

AER	SoS			LoS			$NDVI_{max}$		
	Jun	Jul	Aug	Jun	Jul	Aug	Jun	Jul	Aug
2	-4.47	-7.17	-10.64	4.06	2.87	3.96	0.002	0.058	0.106
3	-6.57	0.04	-0.09	1.71	5.57	-0.34	-0.008	0.015	0.062
4	-5.07	-2.64	-2.14	0.44	0.22	3.50	-0.004	0.030	0.052
5	-12.01	0.60	-3.40	0.38	-1.66	0.77	-0.033	0.006	-0.003
6	-9.54	-2.26	-6.23	2.13	2.67	-1.46	-0.003	0.029	0.029
7	-6.72	-0.64	-8.17	4.77	7.38	3.08	0.024	0.052	0.064
8	-2.36	-0.87	2.92	2.53	5.22	4.73	0.015	0.020	0.049
9	0.59	-1.03	-2.39	4.33	2.61	2.87	0.005	0.019	0.024
10	-5.25	-0.50	-5.79	-2.68	-1.33	0.25	-0.018	0.008	0.002
11	1.38	-2.26	-8.54	-1.06	-0.31	-0.58	0.018	0.038	0.033
12	-0.69	0.78	-11.26	-1.18	0.19	2.67	0.018	0.025	0.023
13	-6.37	-9.19	-11.71	2.85	4.10	6.07	-0.001	0.001	-0.004
14	5.63	-5.36	-10.94	-1.97	-2.29	-0.36	-0.010	0.006	0.008
15	-2.76	-1.27	-1.84	-3.82	0.44	-0.71	-0.012	-0.006	0.000
17	-18.25	-16.23	-3.02	-3.13	2.80	1.74	0.003	0.002	-0.003
18	-3.15	-0.66	-4.89	1.44	2.27	-8.45	-0.007	-0.003	-0.002
19	-8.36	-0.79	3.72	-2.27	0.98	0.86	0.027	0.038	0.040

The sensitivity analysis revealed a rapid increase in sensitivity from arid to semi-arid regions, followed by a decline from semi-humid to humid regions (Piao 2011; Javed et al. 2021). Furthermore, we found that extreme wet or dry years resulted in relatively less change in $NDVI_{max}$ compared to change in the SoS. This finding aligns with the results of other studies (Jiang et al. 2018; Javed et al. 2021). Previous research (Glade et al. 2016; Hao et al. 2019; Stocker 2014) has reported that excessive rainfall can lead to cloudy conditions, thereby obstructing incoming solar radiation and reducing vegetation photosynthesis and plant growth. Therefore, the

effect of the extreme wet conditions on the $NDVI_{max}$ during the peak growth stage is not considerable since crops require ample solar radiation for photosynthesis during this phase (Hao et al. 2019). Pheno-metrics in semi-arid regions exhibited greater sensitivity to wetness and dryness compared to arid regions. This is in contrast with the notion that arid regions, characterized by limited water availability, are more sensitive to climatic variations (Delgado et al. 2018). The reason for this discrepancy may be attributed to the apparent plant acclimatization and resilience to drought conditions due to physiological adaptations (Ma et al. 2015).

4.6 Limitations and challenges

Analyzing the impact of dry and wet events on crop phenology is crucial for comprehending its relationship with climate change. Satellite data can effectively monitor the crop phenology over large areas; however, several limitations and challenges exist in phenology retrieval. Satellite data in monsoon season is often contaminated by cloud and cloud shadows, which introduces uncertainty. Extricating the noise from growth profile and preserving the relevant information proves to be exceedingly difficult. Although various smoothing techniques are available to mitigate noise, selecting the most suitable method that accounts for crop variability over large heterogeneous areas remains a challenge. A recent study by Meroni et al. (2021) explored the use of high-resolution Sentinel-1 data in microwave region and Sentinel-2 data in optical region to map the phenology in Europe using TIMESAT. Future research should focus on joint analysis of multi-source data to study the pheno-metrics while avoiding cloud/noise contamination. Additionally, combining data from optical and microwave sources can be a valuable tool for understanding underlying physiological processes, such as changes in biomass with phenology. Apart from this, the accuracy of outputs is influenced by the pheno-metrics detection method and trend analysis techniques employed. The current detection methods rely on mathematical theories rather than physiological foundations, limiting both understanding and accuracy. Nonetheless, several emerging techniques and sensors offer promising options for future research in exploring the effect of drought events on agriculture.

5 Conclusions

Given the importance of assessing impact of the dryness/wetness condition on crop phenology in the context of climate change, the present study analyzed the spatial patterns and temporal trend of phenological metrics vis-à-vis SPEI-03 as per the prevailing soil and climate resilience. The study has further examined the sensitivity of SPEI-03 derived dryness/wetness patterns to the satellite-derived phenological metrics in agro-ecological zones over India. The SPEI-03 revealed that the hot sub-humid regions were more prone to dryness than semi-arid regions. An increasing trend in dryness was observed in the north-eastern part of India comprising AERs 15, 16, and 17. The SPEI-03 in dry and wet years also revealed an abrupt change in the phenological metrics such as SoS, LoS, and NDVI_{max} in most AERs. As expected, dryness during the early monsoon period delayed SoS, reduced NDVI_{max}, and decreased LoS in most of the AERs. The NDVI_{max} in July and August also showed positive sensitivity towards an increase in wetness. Most of the agricultural area (>50%) showed an increasing trend of SoS and LoS. Drought

resistance to agriculture is more robust in the northwest part of India than in the central and northeast parts. Moreover, SoS exhibited a stronger correlation with SPEI-03 than LoS. The sensitivity of each phenological metric revealed that SoS is sensitive to drought during the monsoon period in almost all AERs. In contrast, NDVI_{max} exhibited much sensitivity towards SPEI-03 in August month. Our results will be helpful in understanding the agricultural crop resilience to drought, decision-making for crop management, and crop insurance in future course of time.

Acknowledgements Authors thank the Director, National Remote Sensing Centre (NRSC), Hyderabad, India and Deputy Director, Remote Sensing Applications, NRSC for providing facility to carry out the work. Authors also acknowledge the support provided by University of Hyderabad (UoH), Hyderabad, India. We acknowledge the NASA Land Processes Distributed Active Archive Center (LP DAAC) for providing MODIS data. Sincere thanks to Prof. P. Jönsson and L. Eklundh for providing the TIMESAT 3.3 program. Thanks to CRU dataset for providing gridded SPEI-03 data.

Author contribution M.K.: conceptualization, methodology, data curation, investigation, formal analysis, writing original draft paper, editing. A.C.: conceptualization, methodology, resources, supervision, writing, review, editing. V.C.: supervision, resources, writing—review, editing. P.S.R.: supervision, writing—review, editing.

Data availability Data are available upon request on the corresponding author.

Declarations

Conflict of interest The authors declare no competing interests.

References

- Ahmad FM, Shen R, Zaheer AB, Ahmad MN, Zhang Y (2018) Study capability of Standardized Precipitation Evapotranspiration Index to represent soil moisture variability during winter season over Pakistan for the period 1951–2010. *Meteorol Atmos Phys* 130(6):689–699
- Anwar MR, Li Liu D, Farquharson R, Macadam I, Abadi A, Finlayson J, Wang B, Ramilan T (2015) Climate change impacts on phenology and yields of five broadacre crops at four climatologically distinct locations in Australia. *Agric Syst* 132:133–144
- Arora NK (2019) Impact of climate change on agriculture production and its sustainable solutions. *Environ Sustain* 2(2):95–96
- Beguéria S, Vicente-Serrano SM, Reig F, Latorre B (2014) Standardized precipitation evapotranspiration index (SPEI) revisited: parameter fitting, evapotranspiration models, tools, datasets and drought monitoring. *Int J Climatol* 34(10):3001–3023
- Bhavani P, Chakravarthi V, Roy PS, Joshi P K, Chandrasekar K (2017) Long-term agricultural performance and climate variability for drought assessment: a regional study from Telangana and Andhra Pradesh states, India. *Geomat Nat Hazards Risk* 8(2):822–840. <https://doi.org/10.1080/19475705.2016.1271831>
- Chakraborty A, Seshasai MV, Dadhwal VK (2014) Geo-spatial analysis of the temporal trends of kharif crop phenology metrics over India and its relationships with rainfall parameters. *Environ Monit Assess* 186(7):4531–4542

- Chakraborty A, Seshasai MV, Rao SV, Dadhwal VK (2017) Geo-spatial analysis of temporal trends of temperature and its extremes over India using daily gridded ($1^\circ \times 1^\circ$) temperature data of 1969–2005. *Theor Appl Climatol* 130(1):133–149
- Chakraborty A, Seshasai MVR, Reddy CS, Dadhwal VK (2018a) Persistent negative changes in seasonal greenness over different forest types of India using MODIS time series NDVI data (2001–2014). *Ecol Indic* 85:887–903
- Chakraborty D, Sehgal VK, Dhakar R, Das DK, Sahoo RN (2018b) Trends and change-point in satellite derived phenology parameters in major wheat growing regions of north India during the last three decades. *J Indian Soc Remote Sens* 46(1):59–68
- Chen H, Sun J (2017) Characterizing present and future drought changes over eastern China. *Int J Climatol* 37:138–156
- Chen J, Jönsson P, Tamura M, Gu Z, Matsushita B, Eklundh L (2004) A simple method for reconstructing a high-quality NDVI time-series data set based on the Savitzky–Golay filter. *Remote Sens Environ* 91(3–4):332–344
- Chen C, Park T, Wang X, Piao S, Xu B, Chaturvedi RK, Fuchs R, Brovkin V, Ciais P, Fensholt R, Myneni RB (2019) China and India lead in greening of the world through land-use management. *Nat Sustain* 2:122–129
- Dalezios NR, Blanta A, Spyropoulos NV, Tarquis AM (2014) Risk identification of agricultural drought for sustainable agroecosystems. *Nat Hazards Earth Syst Sci* 14(9):2435–2448
- Das PK, Chakraborty A, Seshasai MV (2014) Spatial analysis of temporal trend of rainfall and rainy days during the Indian Summer Monsoon season using daily gridded (0.5×0.5) rainfall data for the period of 1971–2005. *Meteorol Appl* 21(3):481–493
- Das PK, Das R, Das DK, Midya SK, Bandyopadhyay S, Raj U (2020) Quantification of agricultural drought over Indian region: a multivariate phenology-based approach. *Nat Hazards* 101(1):255–274
- Das PK, Mohinuddin SK, Midya SK, Das DK, Sharma R, Bandyopadhyay S (2021) Can multiscale meteorological drought indices detect soil moisture droughts? A study of Indian regions. *Hydrol Sci J* 66(9):1475–1487
- De Beurs KM, Henebry GM (2005) Land surface phenology and temperature variation in the International Geosphere–Biosphere Program high-latitude transects. *Glob Chang Biol* 11(5):779–790
- Delgado M, Hidalgo M, Puerta P, Sánchez-Leal R, Rueda L, Sobrino I (2018) Concurrent changes in spatial distribution of the demersal community in response to climate variations in the southern Iberian coastal Large Marine Ecosystem. *Mar Ecol Prog Ser* 607:19–36
- Eklundh L, Jönsson P (2017) TIMESAT 3.3 Software Manual. Lund and Malmö University, Sweden
- Felton AJ, Zavislan-Pullaro S, Smith MD (2019) Semi-arid ecosystem sensitivity to precipitation extremes: weak evidence for vegetation constraints. *Ecol* 100:e02572
- Friedl MA, Gray JM, Melaas EK, Richardson AD, Hufkens K, Keenan TF, Bailey A, O’Keefe J (2014) A tale of two springs: using recent climate anomalies to characterize the sensitivity of temperate forest phenology to climate change. *Environ Res Lett* 9(5):054006
- Fu YH, Piao S, Delpierre N, Hao F, Hänninen H, Liu Y, Sun W, Janssens IA, Campioli M (2018) Larger temperature response of autumn leaf senescence than spring leaf-out phenology. *Glob Chang Biol* 24:2159–2168
- Ge W, Han J, Zhang D, Wang F (2021) Divergent impacts of droughts on vegetation phenology and productivity in the Yungui Plateau, southwest China. *Ecol Indic* 127:107743
- Glade FE, Miranda MD, Meza FJ, van Leeuwen WJ (2016) Productivity and phenological responses of natural vegetation to present and future inter-annual climate variability across semi-arid river basins in Chile. *Environ Monit Assess* 188:676
- Guntukula R (2020) Assessing the impact of climate change on Indian agriculture: evidence from major crop yields. *J Public Aff* 20(1):e2040
- Güsewell S, Furrer R, Gehrige R, Pietragalla B (2017) Changes in temperature sensitivity of spring phenology with recent climate warming in Switzerland are related to shifts of the pre-season. *Glob Chang Biol* 23(12):5189–5202
- Hao Z, Di S, Wu M, Zheng J (2019) Does El Niño play an early signal role for the south-flood north-drought pattern over eastern China? *Theor Appl Climatol* 137:217–227
- Hatfield JL, Prueger JH (2015) Temperature extremes: effect on plant growth and development. *Weather Clim Extrem* 10:4–10
- Heumann BW, Seaquist JW, Eklundh L, Jönsson P (2007) AVHRR derived phenological change in the Sahel and Soudan, Africa, 1982–2005. *Remote Sens Environ* 108(4):385–392
- IPCC, 2021. Masson-Delmotte V, Zhai P, Pirani A, Connors SL, Péan C, Berger S, Caud N, Chen Y, Goldfarb L, Gomis MI, Huang M. Climate change 2021: the physical science basis. Contribution of working group I to the sixth assessment report of the intergovernmental panel on climate change. 2021 Jun;2.
- Ishtiaq M, Maqbool M, Muzamil M, Casini R, Alataway A, Dewidar AZ, El-Sabroun AM, Elansary HO (2022) Impact of climate change on phenology of two heat-resistant wheat varieties and future adaptations. *Plants* 11(9):1180
- Javed T, Li Y, Feng K, Ayantobo OO, Ahmad S, Chen X, Rashid S, Suon S (2021) Monitoring responses of vegetation phenology and productivity to extreme climatic conditions using remote sensing across different sub-regions of China. *Environ Sci Pollut Res* 28(3):3644–3659
- Jeganathan C, Dash J, Atkinson PM (2010) Mapping the phenology of natural vegetation in India using a remote sensing-derived chlorophyll index. *Int J Remote Sens* 31(22):5777–5796
- Jiang Y, Wang R, Peng Q, Wu X, Ning H, Cheng L (2018) The relationship between drought activity and vegetation cover in Northwest China from 1982 to 2013. *Nat Hazards* 92(1):145–163
- Jönsson P, Eklundh L (2004) TIMESAT—a program for analyzing time-series of satellite sensor data. *Comput Geosci* 30(8):833–845
- Kang W, Wang T, Liu S (2018) The response of vegetation phenology and productivity to drought in semi-arid regions of Northern China. *Remote Sens* 10:727
- Kendall M (1976) Rank correlation methods, 4th edn. Griffin, London
- Kumar R, Gautam HR (2014) Climate change and its impact on agricultural productivity in India. *J Climatol Weather Forecast* 2(1):1–3
- Kumar R, Nath AJ, Nath A, Sahu N, Pandey R (2022) Landsat-based multi-decadal spatio-temporal assessment of the vegetation greening and browning trend in the Eastern Indian Himalayan Region. *Remote Sens Appl: Soc Environ* 25:100695
- Li Z, Lyu S, Ao Y, Wen L, Zhao L, Wang S (2015) Long-term energy flux and radiation balance observations over Lake Ngoring, Tibetan Plateau. *Atmos Res* 155:13–25
- Liu X, Pan Y, Zhu X, Yang T, Bai J, Sun Z (2018) Drought evolution and its impact on the crop yield in the North China Plain. *J Hydrol* 564:984–996
- Liu H, Jiao F, Yin J, Li T, Gong H, Wang Z, Lin Z (2020) Nonlinear relationship of vegetation greening with nature and human factors and its forecast—a case study of Southwest China. *Ecol Indic* 111:106009
- Ma X, Huete A, Moran S, Ponce-Campos G, Eamus D (2015) Abrupt shifts in phenology and vegetation productivity under climate extremes. *J Geophys Res Biogeosci* 120:2036–2052
- Malhi GS, Kaur M, Kaushik P (2021) Impact of climate change on agriculture and its mitigation strategies: a review. *Sustain* 13(3):1318
- Mall RK, Singh R, Gupta A, Srinivasan G, Rathore LS (2006) Impact of climate change on Indian agriculture: a review. *Clim Chang* 78(2):445–478. <https://doi.org/10.1007/s10584-005-9042-x>

- Mann HB (1945) Nonparametric tests against trend. *Econometrica: J Econom Soc* 1:245–259
- McKee TB, Doesken NJ, Kleist J (1993) The relationship of drought frequency and duration to time scales. In *Proceedings of the 8th Conference on Applied Climatology*. 17(22):179–183.
- Meroni M, d'Andrimont R, Vrieling A, Fasbender D, Lemoine G, Rembold F, Seguíni L, Verhegghen A (2021) Comparing land surface phenology of major European crops as derived from SAR and multispectral data of Sentinel-1 and-2. *Remote Sens Environ* 253:112232
- Mishra AK, Singh VP (2011) Drought modeling—a review. *J Hydrol* 403(1–2):157–175
- Nam WH, Hayes MJ, Svoboda MD, Tadesse T, Wilhite DA (2015) Drought hazard assessment in the context of climate change for South Korea. *Agric Water Manag* 160:106–117
- NRSC (2014) Land Use/Land Cover Database on 1:50,000 Scale. In: *Natural Resources Census Project*. LUCMD, LRUMG, RSAA, National Remote Sensing Centre, ISRO, Hyderabad
- Palmer WC (1965) Meteorological drought. US Department of Commerce, Weather Bureau
- Parida BR, Pandey AC, Patel NR (2020) Greening and browning trends of vegetation in India and their responses to climatic and non-climatic drivers. *Clim* 8(8):92
- Parsons DJ, Rey D, Tanguy M, Holman IP (2019) Regional variations in the link between drought indices and reported agricultural impacts of drought. *Agric Syst* 173:119–129
- Piao S, Wang X, Ciais P, Zhu B, Wang T, Liu J (2011) Changes in satellite-derived vegetation growth trend in temperate and boreal Eurasia from 1982 to 2006. *Glob Chang Biol* 17:3228–3239
- Potopová V, Štěpánek P, Možný M, Türkott L, Soukup J (2015) Performance of the standardised precipitation evapotranspiration index at various lags for agricultural drought risk assessment in the Czech Republic. *Agric For Meteorol* 202:26–38
- Pramudya Y, Onishi T (2018) Assessment of the standardized precipitation index (SPI) in Tegal City, Central Java, Indonesia. *IOP Conf Ser: Earth Environ Sci* 129(1):012019
- Rai SK, Apoorva SPR (2020) Climate change, pandemic and its impact on Indian agriculture. *Agric Food* 2(10):284–287
- Ranjan AK, Gorai AK (2022) Evaluating phenological trends of different vegetation types in response to climate change over the Rajmahal Hills in India during 2001–2019. *Remote Sens Lett* 13(9):898–911
- Rao CS, Lal R, Prasad JV, Gopinath KA, Singh R, Jakkula VS, Sahrawat KL, Venkateswarlu B, Sikka AK, Virmani SM (2015) Potential and challenges of rainfed farming in India. *Adv Agron* 133:113–181
- Richardson AD, Hollinger DY, Dail DB, Lee JT, Munger JW, O'keefe J (2009) Influence of spring phenology on seasonal and annual carbon balance in two contrasting New England forests. *Tree Physiol* 29(3):321–331
- Sathyan A, Funk C, Anis T, Breuer L (2018) Climate Vulnerability in Rainfed Farming: Analysis from Indian Watersheds. *Sustain* 10(9):3357
- Sehgal VK, Jain S, Aggarwal PK, Jha S (2011) Deriving crop phenology metrics and their trends using times series NOAA-AVHRR NDVI data. *J Indian Soc Remote Sens* 39:373–381
- Sen PK (1968) Estimates of the regression coefficient based on Kendall's tau. *J Am Stat Assoc* 63(324):1379–1389
- Shen M, Tang Y, Chen J, Yang X, Wang C, Cui X, Yang Y, Han L, Li L, Du J, Zhang G (2014) Earlier-season vegetation has greater temperature sensitivity of spring phenology in Northern Hemisphere. *PLoS One* 9(2):e88178
- Shen X, Liu B, Henderson M, Wang L, Jiang M, Lu X (2022) Vegetation greening, extended growing seasons, and temperature feedbacks in warming temperate grasslands of China. *J Clim* 35(15):5103–5117
- Shen X, Jiang M, Lu X (2023) Diverse impacts of day and night temperature on spring phenology in freshwater marshes of the Tibetan Plateau. *Limnol Oceanogr Lett* 8(2):323–329
- Singh S, Sanatan N (2021) Assessment of climate change impact on wheat yield in western dry region: a district level analysis. *Clim Change* 6(21):25–34
- Stocker T (2014) *Climate change 2013: the physical science basis: Working Group I contribution to the fifth assessment report of the Intergovernmental Panel on Climate Change*. Cambridge University Press
- Subramaniam AR (1983) Agro-ecological zones of India. *Theor Appl Climatol* 32(2):329–333
- Tan B, Morisette JT, Wolfe RE, Gao F, Ederer GA, Nightingale J, Pedely JA (2010) An enhanced TIMESAT algorithm for estimating vegetation phenology metrics from MODIS data. *IEEE J Sel Top Appl Earth Obs Remote Sens* 4(2):361–371
- Tirivarombo S, Osupile D, Eliasson P (2018) Drought monitoring and analysis: standardised precipitation evapotranspiration index (SPEI) and standardised precipitation index (SPI). *Phys Chem Earth* 106:1–10
- Vicente-Serrano SM, Beguería S, López-Moreno JI (2010) A multiscale drought index sensitive to global warming: the standardized precipitation evapotranspiration index. *J Clim* 23(7):1696–1718
- Wang H, Wu C, Ciais P, Peñuelas J, Dai J, Fu Y, Ge Q (2020) Overestimation of the effect of climatic warming on spring phenology due to misrepresentation of chilling. *Nat Commun* 11(1):4945
- Wilhite DA, Buchanan-Smith M (2005) Drought as hazard: understanding the natural and social context. *Drought and water crises* 22:3–29
- Yang Y, Tao B, Liang L, Huang Y, Matocha C, Lee CD, Sama M, Masri BE, Ren W (2021) Detecting recent crop phenology dynamics in corn and soybean cropping systems of Kentucky. *Remote Sens* 13(9):1615
- Zhai L, Feng Q, Li Y (2010) Calculation of actual evapotranspiration based on Morton CRAE in Northwest China. *J Irrig Drain* 29(5):33–38

Publisher's note Springer Nature remains neutral with regard to jurisdictional claims in published maps and institutional affiliations.

Springer Nature or its licensor (e.g. a society or other partner) holds exclusive rights to this article under a publishing agreement with the author(s) or other rightsholder(s); author self-archiving of the accepted manuscript version of this article is solely governed by the terms of such publishing agreement and applicable law.